Nickel Ferrite Nanostructures Prepared by DC Reactive Magnetron Sputtering

Atheer J. Raheem, Salar M. Raji

Department of Physics, College of Science, University of Halabja, Kurdistan Region, IRAQ

Abstract

In this work, a magnetic sensor was fabricated from nickel ferrite ($NiFe_2O_4$) nanostructures prepared by closed-field unbalanced dc reactive magnetron sputtering technique at low pressures. The nickel and iron targets were arranged to serve the quantitative aspect of the reaction forming nickel ferrite molecules before deposited on the substrate. Optimum samples were prepared using $Ar:O_2$ gas mixture of 30:70 mixing ratio, total gas pressure of 0.8mbar, discharge voltage of 1.8kV, discharge current of 25mA and inter-electrode distance of 4cm. These samples showed high structural purity as no peaks belonging to other compounds were observed in the x-ray diffraction patterns. The minimum particle size was determined to be 25nm. The average surface roughness of these samples was 0.465nm. The sensor devices fabricated from these samples were characterized to determine the optimum preparation conditions and the minimum magnetic field intensity detected by the fabricated sensor was 38.2G. The main features of the fabricated sensors are high reliability, low production cost and mechanical rigidity.

Keywords: Magnetic sensor; Nickel ferrite; Nanostructures; Plasma sputtering
Received: 17 January 2024; **Revised:** 12 March 2024r; **Accepted:** 19 March 2024; **Published:** 1 April 2024

1. Introduction

A sensor is a device that converts a physical phenomenon into an electrical signal. Such sensors represent part of the interface between the physical world and the electrical and electronic devices, such as control circuits and computers [1]. The highest quality, most up-to-date, most accurately calibrated and most carefully selected sensor can still give totally erroneous data if it is not correctly applied [2,3].

Magnetic sensors are widely used in the field of mineral, navigational, automotive, medical, industrial, military, and consumer electronics [4-7]. Many magnetic sensors have been developed that are generated by specific laws or phenomena: such as search-coil, fluxgate, Hall Effect, anisotropic magnetoresistance (AMR), giant magnetoresistance (GMR), magnetoelectric (ME), magnetodiode, magnetotransictor, fiber-optic, optical pump, superconducting quantum interference device (SQUID), etc. Each of these magnetic field sensors has their merits and application areas [8-12].

Permanent magnetic moments in ferromagnetic materials result from atomic magnetic moments due to uncancelled electron spins as a consequence of the electron structure [13]. There is also an orbital magnetic moment contribution that is small in comparison to the spin moment. Furthermore, in a ferromagnetic material, coupling interactions cause net spin magnetic moments of adjacent atoms to align with one another, even in the absence of an external field [14,15]. All these features make these materials very important to respond to the magnetic fields in their environment as well as to detect magnetic materials [16]. Devices required for these purposes are known as magnetic sensors. These devices are designed and fabricated to detect as low as possible magnetic field strengths and magnetization [17,18].

2. Experimental Part

The dc plasma sputtering system used in this work contains of a vacuum chamber, two discharge electrodes, vacuum pumps and accessories, and cooling and heating facilities. The chamber could be evacuated down to 10^{-3} mbar by a rotary pump and to 10^{-5} mbar by a diffusion pump. The base vacuum was determined by the purpose of

 © All Copyrights are reserved

the discharge process. Argon at maximum pressure of 0.8mbar was used as the discharge gas and its pressure was finely controlled by needle valve. More details on the dc plasma sputtering system can be found in references [19-24].

The inter-electrode distance could be easily varied from 0 to 10cm as the system was operated. The cathode was cooled down to about 10°C to prevent the secondary electron emission while the anode could be heated by an underneath heater or kept at room temperature. The two targets of nickel (Ni, 99.99%) and iron (Fe, 99.9%) were mounted on the cathode with some geometrical arrangement suitable for the work, while the glass substrate on which the films were deposited was placed on the anode. All results presented in this work were obtained by using the concentric arrangement of the Ni and Fe targets.

Highly-pure oxygen gas was flowing to the chamber throughout needle valve to represent the reactive gas required to form the compound of nickel ferrite. The mixture of argon and oxygen gases could be controlled by a gas mixing unit before entering the chamber.

The film thickness was measured by laser fringes method to be about 178 nm for the sample prepared at 4 cm inter-electrode distance, 0.8mbar gas pressure, 30:70 $Ar:O_2$ mixing ratio, 1.8 kV discharge voltage, 25 mA discharge current and deposition time of 4 hours.

The characterization and measurements included x-ray diffraction (XRD), scanning electron microscopy (SEM), atomic force microscopy (AFM) and Fourier-transform infrared (FTIR) spectroscopy

3. Results and Discussion

Figure (1) shows a photograph of the $NiFe_2O_4$ thin films prepared in this work on glass substrates using argon and oxygen gas mixture of 30:70 mixing ratio at different inter-electrode distances (2-7cm). The samples prepared at inter-electrode distance of 4 cm showed the highest homogeneity in the film thickness. Therefore, they were selected to fabricate the magnetic sensor device.

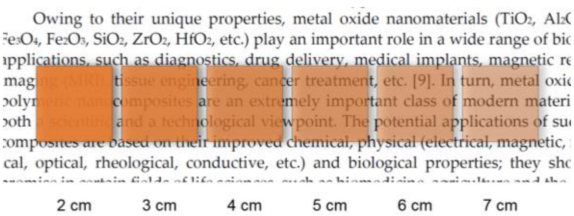

Fig. (1) The $NiFe_2O_4$ thin film samples prepared on glass substrates at different inter-electrode distances using $Ar:O_2$ gas mixture of 30:70 mixing ratio

Figure (2) shows the XRD pattern of the $NiFe_2O_4$ thin film sample prepared at inter-electrode distance of 4cm using $Ar:O_2$ gas mixture of 30:70 mixing ratio. The structure of the sample was determined to be polycrystalline and sharp peaks are observed at diffraction angles of 30.10°, 35.51°, 43.16°, 56.96°, 57.15° and 62.74°. These angles correspond to crystal planes of (220), (311), (400), (422), (511) and (440), respectively. The most dominant crystalline orientation is (311) with approximate grain size of 13nm.

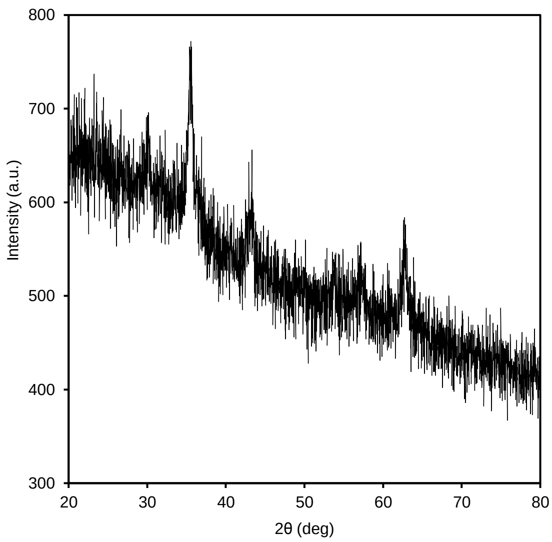

Fig. (2) The XRD pattern of the $NiFe_2O_4$ thin film sample prepared at inter-electrode distance of 4cm using $Ar:O_2$ gas mixture of 30:70 mixing ratio

In the FTIR transmission spectrum of the prepared nanostructured $NiFe_2O_4$ thin film in the range 400-4000 cm^{-1} shown in Fig. (3), two distinct peaks are observed around 430 and 603 cm^{-1}. They are attributed to the octahedral metal stretching vibration (Ni-O) and the tetrahedral metal intrinsic stretching vibration (Fe-O), respectively [3-6]. Other small peaks observed in the range 2400-2800 cm^{-1} are assigned to the stretching modes of the free or adsorbed water.

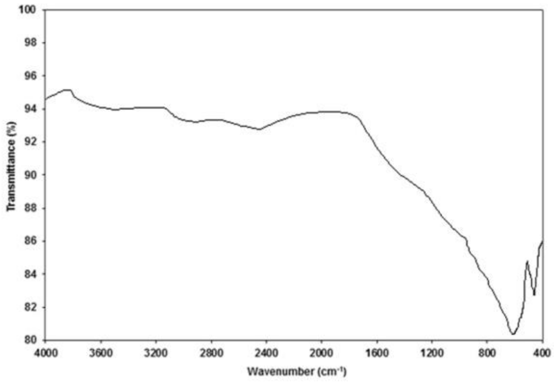

Fig. (3) The FTIR transmission spectrum of the $NiFe_2O_4$ thin film sample prepared at inter-electrode distance of 4cm using $Ar:O_2$ gas mixture of 30:70 mixing ratio

As for most sensing device applications, the surface area is required to be as large as possible, nanostructures are principally satisfying this requirement with surface roughness lower than 5nm. The 3D AFM image of the prepared surface is shown in Fig. (4) and the average roughness is determined to be 0.465nm. Such value can reasonably improve the sensitivity of the prepared surface to the surrounding magnetic fields.

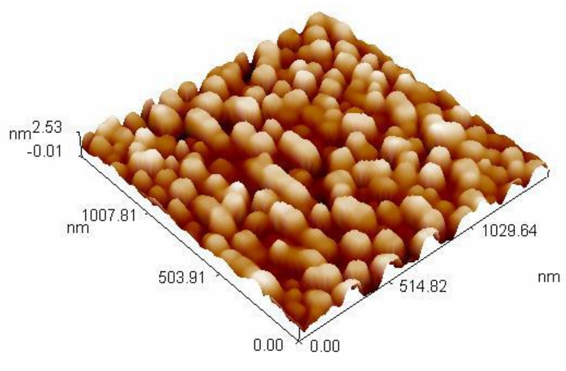

Fig. (4) The 3D AFM image of the $NiFe_2O_4$ thin film sample prepared at inter-electrode distance of 4cm using $Ar:O_2$ gas mixture of 30:70 mixing ratio

The nanostructure of the prepared sample was characterized by SEM as shown in Fig. (5). Minimum particle size of 25nm was determined for the sample prepared at inter-electrode distance of 4cm and $Ar:O_2$ gas mixing ratio of 30:70. The aggregation of nanoparticles can limit their homogeneous sensitivity to the magnetic fields. However, this sample shows the lowest aggregation compared to samples prepared at different inter-electrode distances and mixing ratios.

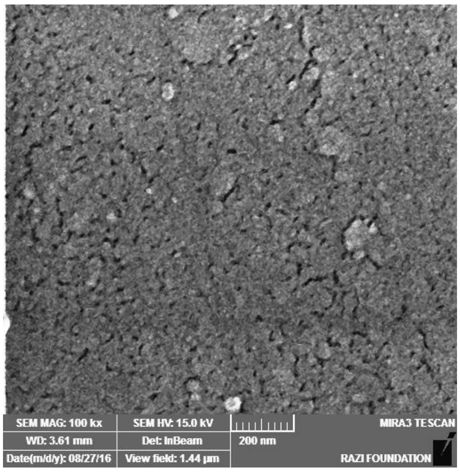

Fig. (5) The SEM image of the $NiFe_2O_4$ thin film sample prepared at inter-electrode distance of 4cm using $Ar:O_2$ gas mixture of 30:70 mixing ratio

4. Conclusions

In concluding remarks, a new arrangement of concentric targets in a closed-field unbalanced magnetron dc reactive co-sputtering technique was used to prepare nanostructured nickel ferrite thin films on glass substrates. Highly-pure polycrystalline structures with dominant orientation in the (311) plane were prepared. Minimum nanoparticle size of 25nm was determined in the sample prepared at inter-electrode distance of 4cm and $Ar:O_2$ gas mixing ratio of 30:70. An average roughness of 0.465nm was determined for the same sample.

References

[1] F.J. Al-Maliki, O.A. Hammadi and E.A. Al-Oubidy, “Optimization of Rutile/Anatase Ratio in Titanium Dioxide Nanostructures prepared by DC Magnetron Sputtering Technique”, Iraqi J. Sci., 60 (2019) 91-98.

[2] J. Dresner and F.V. Shallcross, “Crystallinity and Electronic Properties of Evaporated CdS Films”, J. Appl. Phys., 34(8) (1963) 2390.

[3] Oday A. Hamadi, Khaled Z. Yahiya, “Optical and electrical properties of selenium-antimony heterojunction formed on silicon substrate”, Sharjah Univ. J. Pure Appl. Sci. (UoS J PAS), 4(2), 2007, 1-11.

[4] Oday A. Hamadi, Ban A.M. Bader, Afnan K. Yousif, "Electrical Characteristics of Silicon p-n Junction Solar Cells Produced by Plasma-Assisted Matrix Etching Technique", Eng. Technol. J., 28, 2008, 995-1001.
[5] O.A. Hammadi, F.J. Al-Maliki and E.A. Al-Oubidy, "Photocatalytic Activity of Nitrogen-Doped Titanium Dioxide Nanostructures Synthesized by DC Reactive Magnetron Sputtering Technique", Nonlinear Opt. Quantum Opt., 51 (1-2) (2019) 67-78.
[6] Afnan K. Yousif, Oday A. Hamadi, "Plasma-Induced Etching of Silicon Surfaces", Bulg. J. Phys., 35(3), 2008, 191-197.
[7] Oday A. Hamadi, "Characteristics of CdO-Si Heterostructure Produced by Plasma-Induced Bonding Technique", Proc. IMechE, Part L, J. Mater.: Design and Applications, 222, 2008, 65-71, DOI: 10.1243/14644207JMDA56.
[8] Oday A. Hamadi, "Effect of Annealing on the Electrical Characteristics of CdO-Si Heterostructure Produced by Plasma-Induced Bonding Technique", Iraqi J. Appl. Phys. (IJAP), 4(3), 2008, 34-37.
[9] Aseel A.K. Hadi, Oday A. Hamadi, "Optoelectronic Characteristics of As-doped Silicon Photodetectors Produced by LID Technique", Iraqi J. Appl. Phys. Lett. (IJAPLett), 1(2), 2008, 23-26.
[10] Oday A. Hammadi, "Photovoltaic Properties of Thermally-Grown Selenium-Doped Silicon Photodiodes for Infrared Detection Applications", Photonic Sensors, 5(2), 2015, 152-158, DOI: 10.1007/s13320-015-0241-4
[11] Oday A. Hammadi, Mohammed K. Khalaf, Firas J. Kadhim, "Silicon Nitride Nanostructures Prepared by Reactive Sputtering Using Closed-Field Unbalanced Dual Magnetrons", Proc. IMechE, Part L, J. Mater.: Design and Applications, Accepted for publication: July 2015, DOI: 10.1177/1464420715601151.
[12] Oday A. Hammadi, Mohammed K. Khalaf, Firas J. Kadhim, "Fabrication of UV Photodetector from Nickel Oxide Nanoparticles Deposited on Silicon Substrate by Closed-Field Unbalanced Dual Magnetron Sputtering Techniques", Opt. Quantum Electron., 47(12), 2015, 3805-3813. DOI: 10.1007/s11082-015-0247-6
[13] Oday A. Hammadi, Mohammed K. Khalaf, Firas J. Kadhim, "Fabrication and Characterization of UV Photodetectors Based on Silicon Nitride Nanostructures Prepared by Magnetron Sputtering", Proc. IMechE, Part N, J. Nanoeng. Nanosys., accepted for publication: September 3rd 2015.
[14] O.A. Hammadi, M.K. Khalaf, F.J. Kadhim, B.T. Chiad, "Operation Characteristics of a Closed-Field Unbalanced Dual-Magnetrons Plasma Sputtering System", Bulg. J. Phys., 41(1) (2014) 24-33.
[15] O.A. Hammadi, "Production of Nanopowders from Physical Vapor Deposited Films on Nonmetallic Substrates by Conjunctional Freezing-Assisted Ultrasonic Extraction Method", Proc. IMechE, Part N, J. Nanomater. Nanoeng. Nanosys., 232(4) (2018) 135-140.